Modeling of subduction components in the Genesis of the Meso-Cenozoic igneous rocks from the South Shetland Arc, Antarctica

Adriane Machado[a,*], Farid Chemale Jr.[a], Rommulo V. Conceição[a], Koji Kawaskita[a], Diego Morata[b], Orlando Oteíza[b], William R. Van Schmus[c]

[a]*Federal University of Rio Grande do Sul, Institute of Geosciences, Isotope Geology Laboratory, Av. Bento Gonçalves, 9500, Campus do Vale, Agronomia, 91501-970, Porto Alegre, RS, Brazil*
[b]*Department of Geology, University of Chile, Casilla 13518, Correo 21, Santiago, Chile*
[c]*Department of Geology, University of Kansas, Lawrence, KS 66045, USA*

Abstract

Isotope data and trace elements concentrations are presented for volcanic and plutonic rocks from the Livingston, Greenwich, Robert, King George and Ardley islands (South Shetland arc, Antarctica). These islands were formed during subduction of the Phoenix Plate under the Antarctica Plate from Cretaceous to Tertiary. Isotopically $(^{87}Sr/^{86}Sr)_o$ ratios vary from 0.7033 to 0.7046 and $(^{143}Nd/^{144}Nd)_o$ ratios from 0.5127 to 0.5129. εNd values vary from +2.71 to +7.30 that indicate asthenospheric mantle source for the analysed samples. $^{208}Pb/^{204}Pb$ ratios vary from 38.12 to 38.70, $^{207}Pb/^{204}Pb$ ratios are between 15.49 and 15.68, and $^{206}Pb/^{204}Pb$ from 18.28 to 18.81. The South Shetland rocks are thought to be derived from a depleted MORB mantle source (DMM) modified by mixtures of two enriched mantle components such as slab-derived melts and/or fluids and small fractions of oceanic sediment (EM I and EM II). The isotopic compositions of the subduction component can be explained by mixing between at least 4 wt.% of sediment and 96 wt.% of melts and/or fluids derived from altered MORB.

Keywords: Subduction; Fluids; Island arc magmas; Pb isotopes; Nd isotopes; Sr isotopes

1. Introduction

Island arcs are central to the understanding of mantle evolution because they represent the site where crustal material of various types may be returned to

* Corresponding author. Tel.: +55 51 33166398; fax: +55 51 33166340.
E-mail address: adrianemachado@yahoo.com.br (A. Machado).

the deep mantle. Island-arc magmatism may allow us to sample this material that is in the process of being recycled.

White and Dupre (1986) and Ellam and Hawkesworth (1988) proposed three component-mixing models for the island arcs mantle evolution. These involve contamination of the depleted-mantle source of IAB with partial melts of subducted sediment and large-ion lithophile element-enriched slab-derived fluids. Evidence for such a process is seen when abundances of low-field-strength large-ion lithophile elements (LILE), such as Cs, Rb, Ba, Sr, are normalized against high-field-strength elements (HFSE), such as Nb, Zr, Hf, Y. This argument is based on the ratios of mobile and immobile elements in aqueous fluids, ratios of LILE, HFSE and light rare earth elements (Ishikawa and Nakamura, 1994; Ryan et al., 1995; Scambelluri and Philippot, 2001).

The South Shetland Islands arc (Fig. 1) provides an opportunity to compare and contrast the effects of fluids and sediment involvement in a subduction zone. The rocks from the South Shetland Islands are apparently uncontaminated by intra-crustal components and they should have largely evolved through simple fractional crystallization from a primitive island arc basalt precursor. These samples are similar in most aspects to typical island arc rocks, which constitute the bulk of the worldwide database for subduction-related compositions.

In this paper, Sr, Nd and Pb isotopic ratios, together with trace element compositions are presented from samples of the South Shetland Islands. We use these data to discuss the South Shetland Arc mantle source and processes of magma genesis. The studied samples were collected at western Livingston Island (Byers Peninsula, Fig. 2), southeastern Greenwich Island (Fort Point, Fig. 3), western Robert Island (Coppermine Peninsula, Fig. 4), southwestern King George Island (Fildes Peninsula, Fig. 5) and northeastern Ardley Island (Fig. 5). The ages from the South Shetland samples vary from 143 Ma to 44 Ma. (Grikurov et al., 1970; Gracanin, 1983; Smellie et al., 1984; Hathway, 1997; Oteiza, 1999; Pankhurst et al., 2000).

2. Geological setting

The continent of Antarctica is divided into two large geologic areas: East and West Antarctica. East Antarctica is the large bean-shaped land mass centered on 90° east longitude. West Antarctica is the area centered on 90° west longitude and includes the Antarctica Peninsula.

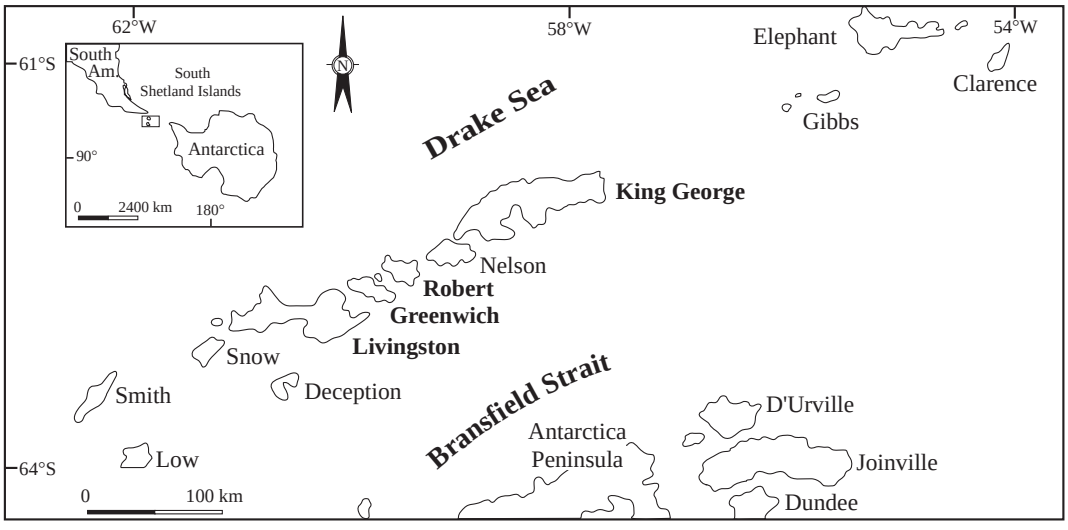

Fig. 1. Location map of the South Shetland Islands (modified from Machado, 1997).

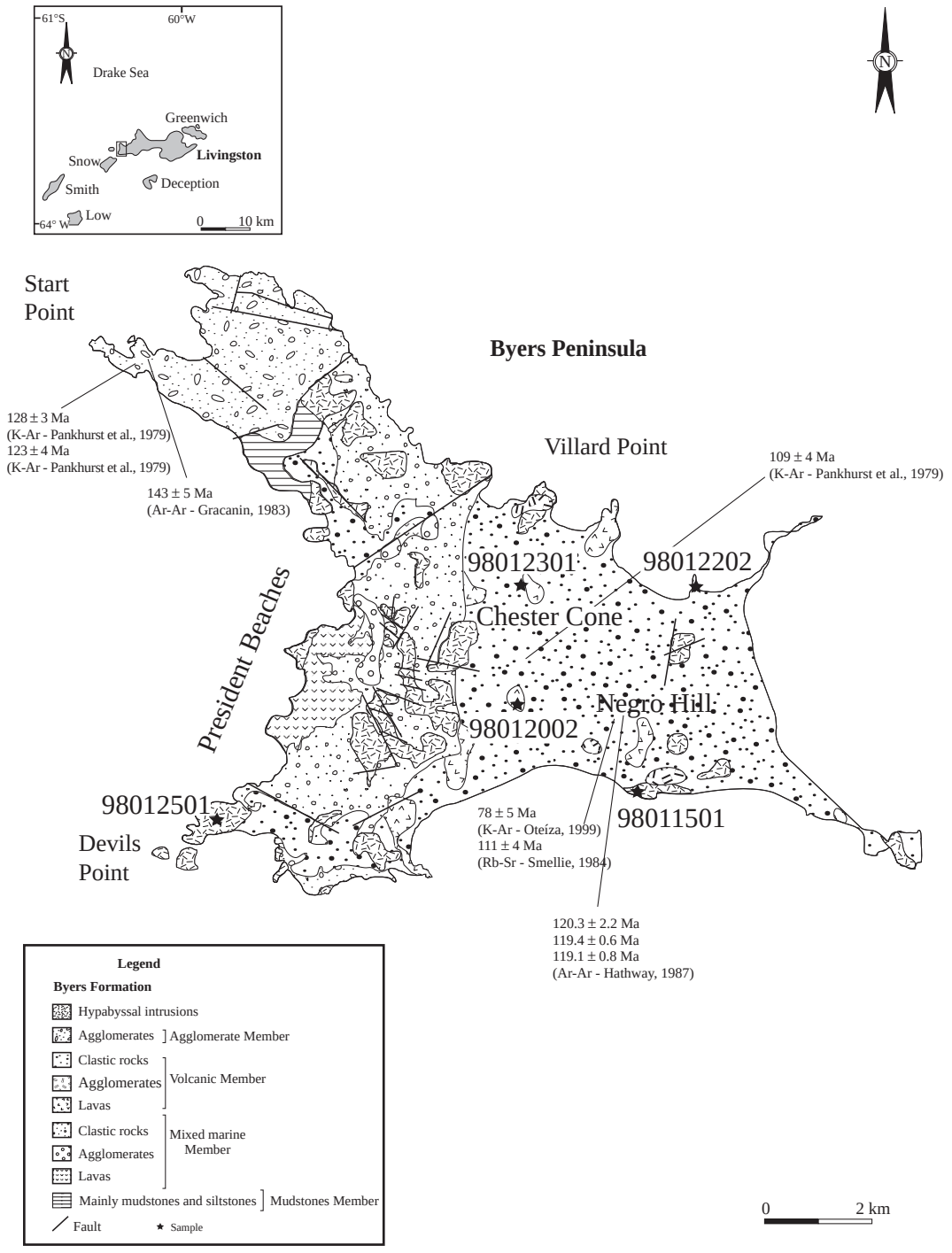

Fig. 2. Sketch of the geological map of Byers Peninsula (Livingston Island) showing sample locations and age of the studied rocks (modified from Smellie et al., 1984).

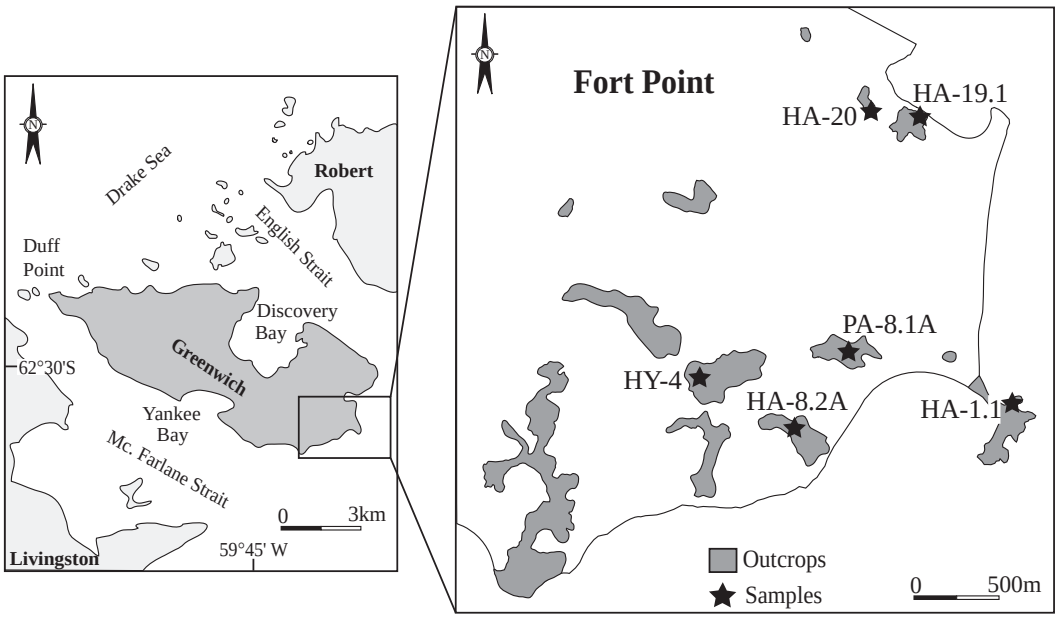

Fig. 3. Sketch of the geological map of Fort Point (Greenwich Island) showing sample locations of the rocks (modified from Azevedo, 1992).

East Antarctica is a large Precambrian shield; a stable portion of a continent composed of old rocks that have changed very little over a long time. The oldest rocks found in this area are over 3 billion years old. These are metamorphic rocks overlaid by younger, flat-lying ocean-deposited sediment. The rocks were recrystallized during a mountain building episode caused by plate collision, in the early Paleozoic Era (about 500 Ma).

West Antarctica was built up over the last 500 million years by the addition of small continental fragments (microplates) that have built up the mountains of West Antarctica. Unlike East Antarctica, if the ice were removed in the west, the land would have considerable relief. The area would probably appear as a series of island chains and mountain ranges.

The Antarctica Peninsula and the rest of West Antarctica were the most recent additions. The Andean Orogeny of late Mesozoic and early Cenozoic (about 60–80 million years ago) formed the peninsula. This activity coincided with the final breakup of Gondwana as South America, Australia, and Antarctica split apart. The peninsula is an extension of the Andes of South America, and likewise these mountains, is made of igneous intrusive and volcanic as well as metamorphosed sedimentary rocks.

The Antarctica Peninsula is bordered by a complex system of tectonic plates, including the South America, Scotia, Drake/Phoenix, South Orkney and Sandwich plates, which are dominated by extensional and strike-slip tectonic limits (Fig. 6). This configuration was formed only in the last 38 Ma with the opening of Drake Passage and Scotia Sea (Barker and Burrell, 1977; Barker et al., 1991). Before 38 Ma the relationships between the major plates were marked by destructive plate interaction generating Mesozoic–Cenozoic accretionary wedges, island arcs and back-arc basins recorded at the South Shetland Islands, Antarctic Peninsula and Patagonia (Dalziel, 1984; Lawver et al., 1996).

The tectonic context of the South America-Scotia-Antarctic plate junction has been related to a complex evolution from Paleozoic–Mesozoic to the present. This evolution is marked by several tectonic episodes from 250 Ma to 20 Ma, such as the Paleozoic–Mesozoic Samfrau Orogeny, early processes of Gondwana fragmentation, Gondwana break-up, Phoenix plate subduction, arc volcanism in the South

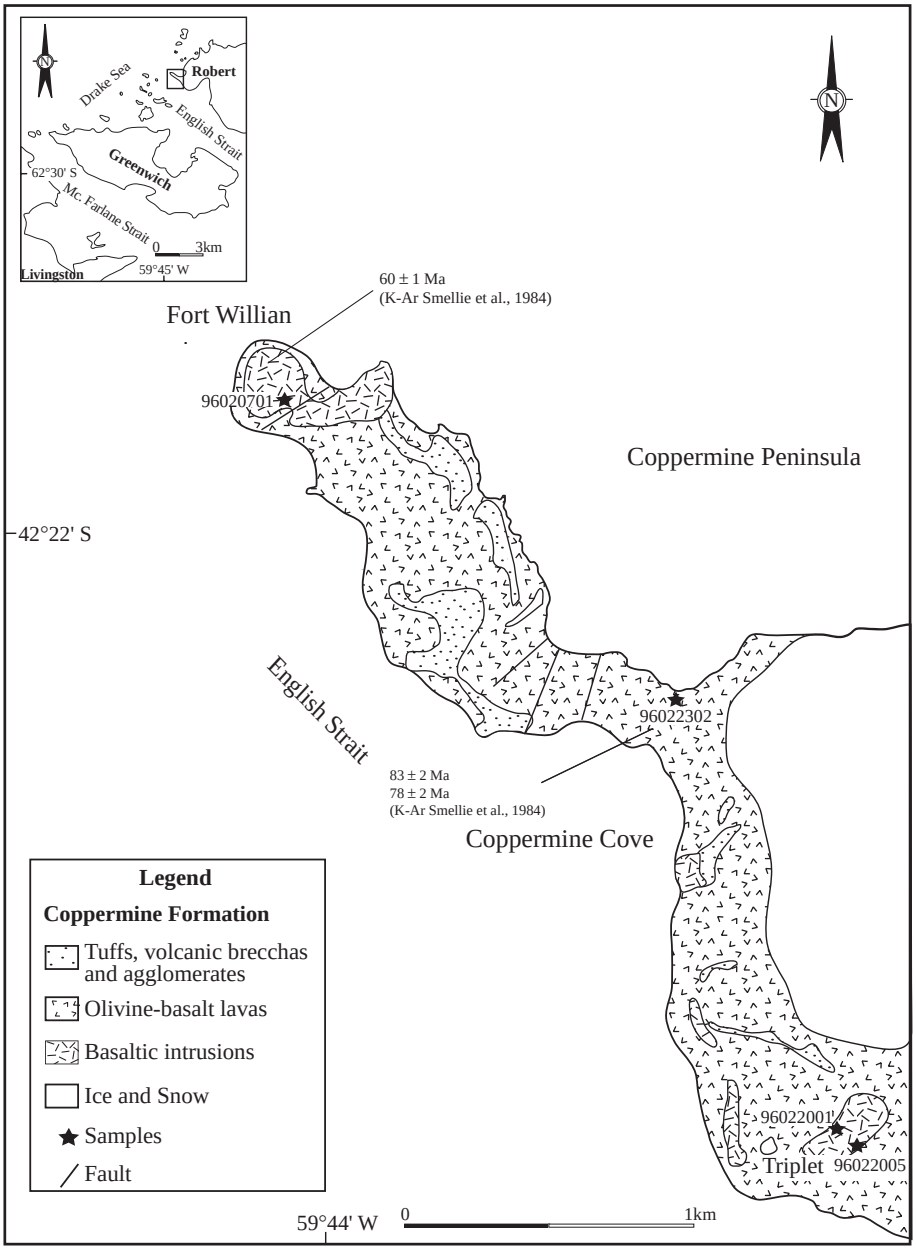

Fig. 4. Sketch of the geological map of Coppermine Peninsula (Robert Island) showing sample locations and age of rocks (modified from Smellie et al., 1984).

Shetland Islands, and extensional tectonism in the Antarctica Peninsula.

The collision of a spreading centre at the Antarctica Peninsula trench caused the migration of magmatism along Antarctica Peninsula from Palmer and Graham lands to South Sandwich Arc where four phases of island arc volcanism have been identified: 130–110 Ma; 90–70 Ma; 60–40 Ma; 30–20 Ma (Birkenmajer et al., 1986). The last two phases define the end of compressive arc at the Shetland Islands through

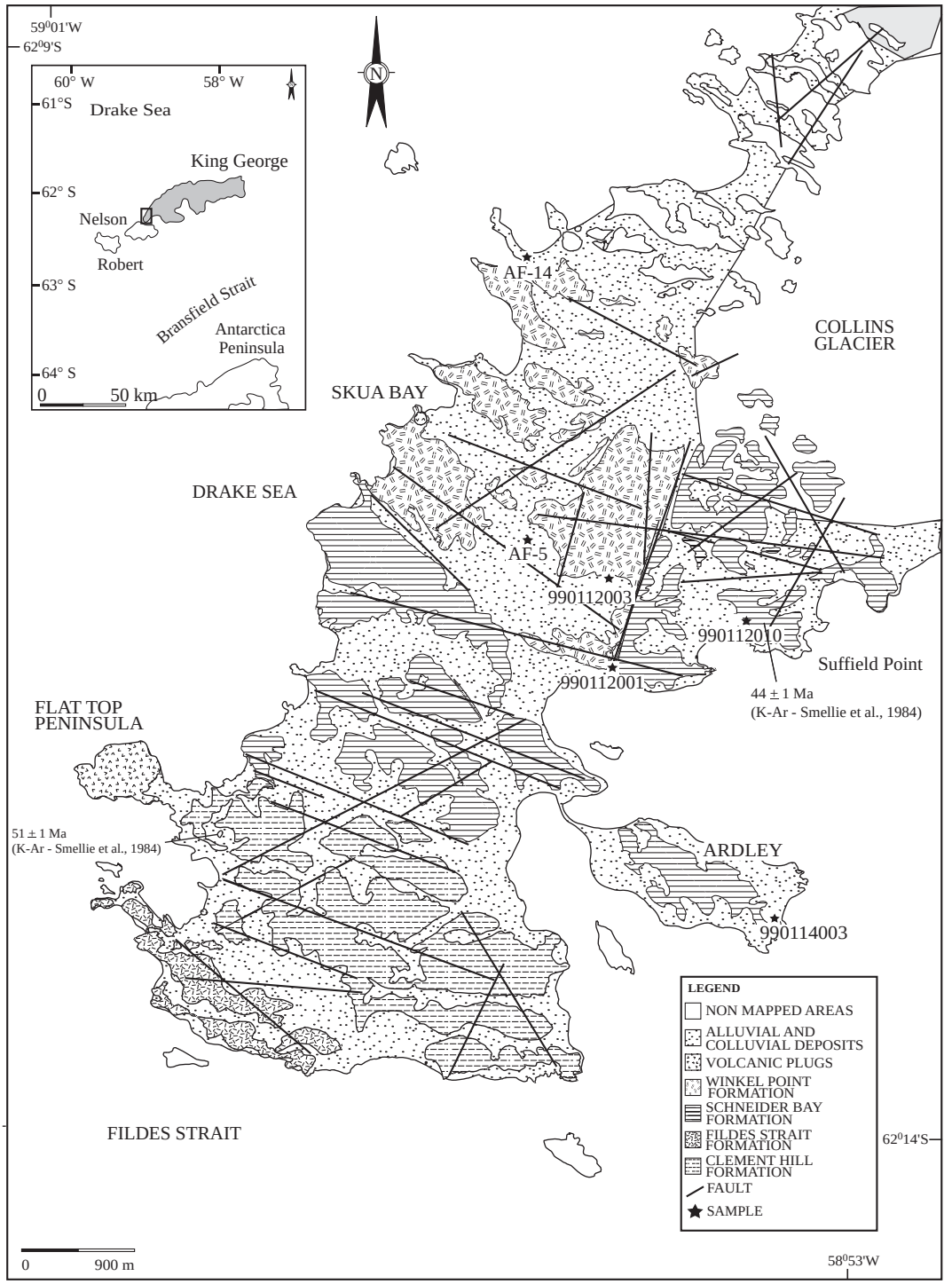

Fig. 5. Sketch of the geological map of Fildes Peninsula (King George Island) and Ardley Island, showing sample locations and age of rocks (modified from Machado, 1997).

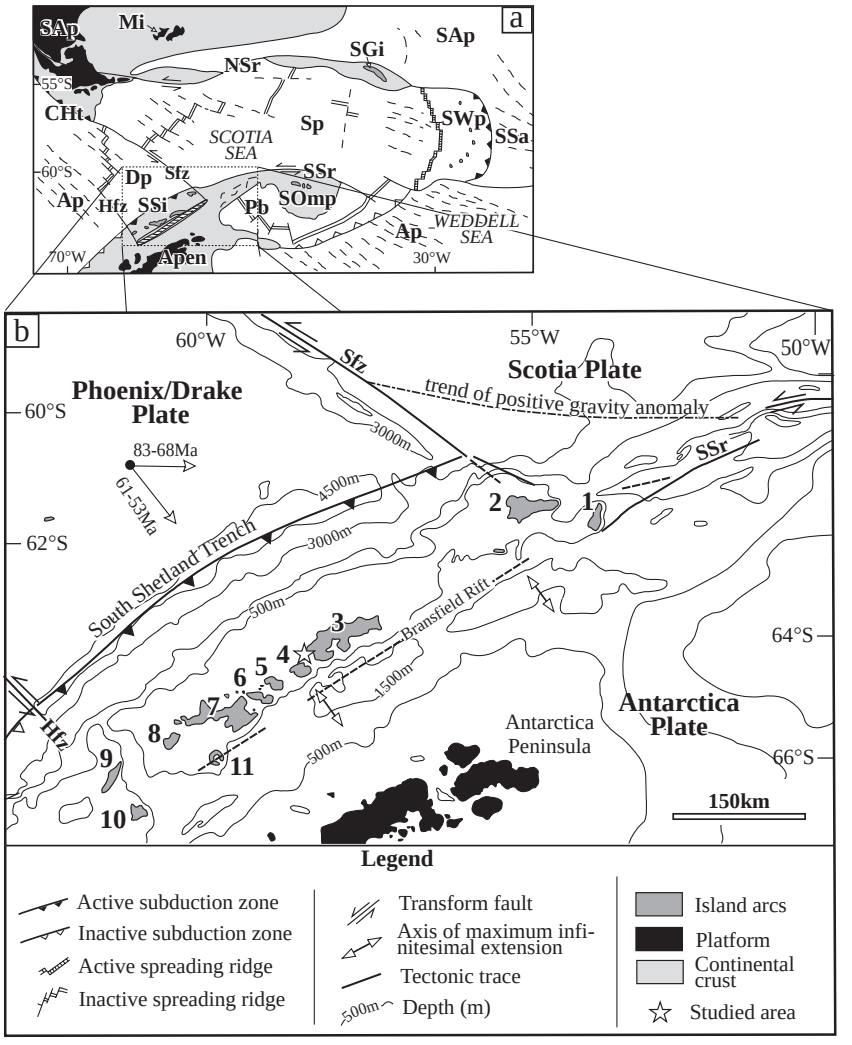

Fig. 6. (a) Geotectonic map of southern of South Atlantic showing the distribution of main tectonic plates—SAp: South America Plate; Sp: Scotia Plate; Ap: Antarctica Plate; SOmp: South Orkney Microplate; SWp: Sandwich Plate; Dp: Drake Plate and features; Mi: Malvinas Islands; CHt: Chile Trench; SGi: South Georgia Island; SSa: South Sandwich Arc; NSr: North Scotia Ridge; SSr: South Scotia Ridge; Pb: Powell Basin; SSi: South Shetland Islands; Hfz: Hero Fault Zone and Sfz: Shackleton Fault Zone (modified from Trouw et al., 2000). (b) Tectonic setting of the South Shetland. Arc islands are represented by the following islands: Clarence (1); Elephant (2); King George (3); Nelson (4); Robert (5); Greenwich (6); Livingston (7); Snow (8); Smith (9) and Low (10) (modified from Lawver et al., 1996). Arrows indicate direction of plate motion in the Cretaceous and Tertiary (McCarron and Larter, 1998).

tholeiitic to calc-alkaline magmatism reported in King George Island (Smellie et al., 1984; Jwa et al., 1991; Machado, 1997).

The South Shetland Islands form a 550 km long archipelago at the southwestern end of the Scotia Ridge, an arcuate structure of islands and submerged continental blocks linking southern South America to the Antarctic Peninsula. That archipelago is on a small crustal plate (Shetland microplate) between South Shetland trench (>5 km deep) and Bransfield Strait, a back arc basin (Keller et al., 1991).

Antarctica is currently tectonically stable in that it experiences little or no volcanism, earthquakes, and is not in motion.

3. Studied samples and petrography

The samples used in this paper were collected during Brazilian and Chilean expeditions to the South Shetland Islands. The main characteristics of the samples are summarized below.

3.1. Plutonic rocks

Plutonic rocks used in this study are from Greenwich Islands. We did not find plutonic rocks in other islands during the fieldtrips.

The gabbro from Fort Point (sample PA-8.1A) is a fine-grained rock consisting essentially of plagioclase, augite and olivine. The plagioclase is mainly labradorite and bytownite with rather irregular or rounded outlines. Albite twinning is very common. Augite ($Wo_{23–48}$; $En_{40–58}$; $Fs_{9–21}$) is greenish, rarely shows concentric zoning and occasionally displays twin lamellae. Olivine (Fo_{71} to Fo_{82}) in most cases is altered to bowlingite or iddingsite, often with bands of dark magnetite granules along its cleavages and cracks. The groundmass is composed of lath-shaped plagioclase, augite, olivine, and accessory minerals (apatite, magnetite, ilmenite).

Tonalites (samples HA-8.2A, HA-20, HY-4) are composed of phenocrysts of plagioclase associated with brown biotite and hornblende in nearly equal proportions, and a small number of opaque minerals. The hornblende is green, sometimes with a tinge of brown; the biotite is always brown and strongly pleochroic. Often these two minerals are clustered together irregularly or in parallel growths. Both of them alter into chlorite, epidote and carbonates. Quartz occurs as irregular simple grains. Accessory minerals are apatite and zircon.

3.2. Volcanic rocks

Among the studied volcanic rocks, porphyritic types are dominant, while aphyric rocks are rare. Basaltic lavas usually contain subhedral-anhedral phenocrysts of plagioclase, augite, and olivine set in a groundmass of plagioclase, augite, olivine and opaque minerals. Rare orthopyroxene may be present and all phenocryst minerals show signs of magmatic resorption, which is more common in plagioclase that frequently shows finger-like features consisting of blebs of dark brown glass. Altered olivine occurs only in basalts and basaltic andesites, whereas orthopyroxene is only present in the basaltic andesites. Almost all samples from Robert Island present well preserved olivine phenocrysts. Glomeroporphyritic clusters are common in the youngest rocks. The matrix exhibits pilotaxitic, intergranular and intersertal textures, and is composed of lath-shaped plagioclase microlites, pyroxene grains, opaque minerals and green-yellow or green-brown alteration material. Pigeonite is rarely present and there may be some micro-phenocrysts of opaque minerals; dark brown glass and green-brown alteration material sometimes occur interstitially. Weathering and formation of clay minerals, such as bowlingite and smectite, caused high LOI in some samples, which were excluded from this chemical and isotopic study.

4. Geochemistry

4.1. Analytical methods

Whole-rock samples were analyzed for major and trace elements by X-ray fluorescence (XRF) at the Department of Geology and Geophysics, University of Adelaide, Australia. Selected trace elements were analyzed by inductively coupled plasma mass spectrometry (ICP-MS) at the Institute of Energetic and Nuclear Research-IPEN, São Paulo, Brazil according to the Figueiredo and Marques (1989) methodology. All samples were crushed in a WC jaw crusher after removal of weathered rims. LOI was determined on approximately four grams of pre-dried sample by heating to 960 °C overnight. Major elements were determined on fused glass discs of sample mixed with lithium meta/tetraborate flux (ratio sample: flux=1/4) with a Philips PW 1480 100 kV spectrometer. Trace elements were analyzed on pressed powder pellets. Reproducibility is generally better than 1% for major elements and around 5% for trace elements. Accuracy of the measurements, as determined by analyses of international standards, is better than 5% for all

elements, except for Ba, Ni, Zn, Cu, Cr, for which accuracy is better than 10%. REE were determined by ICP-MS at ACTLABS, Canada.

Isotope determinations were carried out at the Isotope Geochemistry Laboratory of University of Kansas (UK), USA, and at the Isotope Geology Laboratory (IGL), Federal University of Rio Grande do Sul (UFRGS), Brazil.

Rock powders for Rb–Sr and Sm–Nd analysis were dissolved in Teflon bombs in a microwave using an HF–HNO_3 mixture and 6 N HCL with spike ^{87}Rb–^{84}Sr and ^{149}Sm–^{150}Nd (UK) and without spike (IGL). Sr and REE were extracted using a standard AG-50W cation resin; Sm and Nd were extracted using HDEHP-coated Teflon powder.

Rb was loaded on a single Ta filament with H_3PO_4 and analyzed in static mode. Sr was loaded on a single Ta filament with H_3PO_4. Isotopic compositions were measured with a VG Sector multicollector mass spectrometer using dynamic mode (UK) and static mode (IGL). All analyses are adjusted due to periodic adjustment of collector positions as monitored by measurements of an internal laboratory; which yielded the following values: SRM987=0.710262±0.000023 (n=47, IGL), and 0.710253±0.000024 (n=12, UK).

Sm was loaded on a single Ta filament with H_3PO_4 and analyzed as Sm^+ using static multicollector. Nd was loaded with phosphoric acid on a single Re filament having a thin layer of AGW-50 resin beads and analyzed as Nd^+ using dynamic mode at the UK and on triple Ta-Re-Ta filament using static mode at the IGL. We normally determine 100 ratios with a 1-V ^{144}Nd beam. External precision based on repeated analyses of our internal standard is ±20 ppm (1 standard deviation); all analyses are adjusted for variations instrumental bias due to periodic adjustment of collector positions as monitored by measurements of an internal laboratory standard. This yields La Jolla Nd isotopic ratio=0.51186±0.000020 (UK) and 0.51185±0.000029 (IGL). Sm–Nd ratios were corrected to within ±0.5 percent, based on analytical uncertainties. εNd (t=crystallization age) values were calculated using Ar–Ar and K–Ar ages (Table 2) taken from the literature.

During the course of the analyses Sr, Nd and Sm blanks were lesser than 1.5 ng, 500 pg and 100 pg, respectively.

For the Pb isotopic measurements, an aliquot of 1 ml from dissolved WR samples used for Sr and REE analysis has been taken. Pb was extracted with ion-exchange techniques, with AG-1 ×8, 200–400 mesh, anion resin. Isotopic analyses of Pb composition were carried out with VG Sector mass spectrometer of UK and IGL. Samples were loaded on single Re filaments with silica gel and H_3PO_4. Pb isotopic ratios were corrected to a fractionation factor of 0.13% amu, based on successive determinations of NBS981 and NBS882 common Pb standards. External variations in isotopic ratios are normally 0.1% or lower, based on repeated analyses of NBS981 and NBS982 standards.

4.2. Results

Major and trace element concentrations of the studied samples are given in Table 1. The rocks have variable SiO_2 ranging from ~46 to 64 wt.%, MgO from ~2 to 9 wt.%) and moderate to very high Al_2O_3 contents from ~15 to 26 wt.% that probably reflect variations in the plagioclase modal compositions.

Most samples have low Cr and Ni, indicating they have undergone significant fractional crystallization from mantle-derived melts.

All of the South Shetland samples are enriched in Rb, Ba, K and Sr relative to N-MORB, but they are depleted in Nb, Zr, Hf and Ti (Fig. 7). All samples show positive Ba and Sr anomalies, and pronounced negative Nb and Ti anomalies. On average, the rocks have depleted HFSE characteristics, and enrichment in light and middle REE compared to N-MORB.

All the analyzed samples have chondrite-normalized patterns enriched in LREE relative to HREE, similar to calc-alkaline suites, with $(Ce/Yb)_N$ ranging from 5 to 19 and $(Gd/Lu)_N$>3. The relatively low Yb_N values in all rocks under consideration point to residual garnet in the source.

Nb and Ti show strong negative troughs, and HFSE are less abundant than LILE, relative to N-MORB (Fig. 7) suggesting that the mantle source underlying the Cretaceous–Tertiary South Shetland Islands arc could be a depleted MORB. Stability of Nb-rich phases in the mantle may explain the ubiquitous depletion of Nb in arc-related magmas (Woodhead et al., 1993).

Table 1
Selected major and trace elements whole-rock analyses and ages of the studied plutonic and volcanic rocks from the South Shetland Islands

Sample	Lithology	Age	SiO_2	TiO_2	Al_2O_3	FeO^T	MgO	MnO	CaO	Na_2O	K_2O	P_2O_5	LOI	Total	Rb	Ba	Sr	Ni	Cr	Co	Nb	Zr
Ardley and King George Islands																						
990114003	basaltic andesite	58	53.71	0.70	18.91	9.58	3.72	0.14	7.78	3.74	0.84	0.23	0.84	100.18	11	257	696	4	2	23	2.0	65
990112001	basalt	58	46.91	0.62	23.15	7.83	4.61	0.16	10.99	2.66	0.51	0.09	2.54	100.08	6	263	672	16	13	35	0.4	29
990112003	andesite	44	55.39	0.70	19.19	8.81	2.90	0.16	7.34	4.06	0.92	0.22	0.36	100.06	17	242	615	3	1	31	1.0	98
990112010	basaltic andesite	58	54.16	0.78	19.08	8.03	3.70	0.20	8.48	3.14	0.91	0.21	1.29	100.00	23	280	593	21	50	31	4.5	100
AF-5	basalt	58	50.34	0.45	20.56	7.59	6.15	0.12	10.90	2.16	0.79	0.09	1.78	100.93	11	155	609	6	105	33	1.0	54
AF-14	basalt	58	50.19	0.84	19.89	9.64	4.31	0.18	9.97	3.31	0.57	0.13	1.01	100.04	5	149	575	88	59	31	1.0	44
Greenwich Island																						
HA-1.1	basalt	98	47.47	0.83	25.74	8.67	3.06	0.12	9.33	3.23	0.45	0.04	2.01	100.95	10	184	687	23	82	23	1.0	44
HA-8.2A	tonalite	80	58.69	0.69	17.62	6.74	2.85	0.11	6.97	3.75	1.63	0.19	0.63	99.87	45	340	570	8	30	15	4.6	108
HA-19.1	basalt	98	56.22	0.45	17.10	6.70	4.78	0.12	8.54	2.95	1.05	0.20	1.96	100.18	25	263	491	5	31	n.d.	5.0	235
HA-20	tonalite	80	63.80	0.53	15.58	5.30	2.19	0.12	4.36	3.93	2.05	0.15	1.43	99.46	57	395	443	7	36	12	4.1	157
HY-4	tonalite	80	60.70	0.82	15.90	7.30	2.60	0.12	5.70	3.60	2.70	0.19	0.70	100.30	79	486	412	28	69	19	7.5	176
PA-8.1A	gabbro	80	50.00	0.72	16.80	9.20	7.40	0.16	10.40	2.80	0.50	0.15	1.40	99.50	7	202	533	34	208	32	2.0	53
Livingston Island																						
98011501	basalt	115	49.50	1.42	15.90	12.80	4.20	0.18	9.30	3.60	0.62	0.21	2.30	100.30	8	75	461	15	27	60	1.0	67
98012002	basalt	130	49.60	1.31	17.30	11.60	4.10	0.18	9.30	3.90	0.33	0.28	1.80	100.50	5	126	476	15	20	22	1.0	60
98012202	basalt	115	48.40	0.91	18.29	9.24	7.59	0.16	11.51	2.37	0.42	0.18	1.17	100.25	5	295	574	15	115	49	1.0	40
98012301	andesite	130	57.96	1.31	15.07	9.46	2.36	0.19	6.42	3.72	0.66	0.39	2.15	99.71	25	329	438	15	20	34	3.0	159
98012501	basaltic andesite	130	53.88	1.02	19.63	8.34	2.79	0.13	8.80	3.97	0.96	0.13	2.36	102.01	22	176	369	6	10	22	5.0	82
Robert Island																						
96020701	basalt	82	48.09	0.97	16.93	9.50	8.86	0.14	10.03	2.66	0.58	0.35	1.63	99.73	13	327	538	154	455	41	2.0	76
96022001	basalt	82	49.31	0.89	17.50	9.60	8.00	0.17	10.82	2.51	0.21	0.15	1.08	100.24	3	122	482	100	329	47	1.0	42
96022005	basalt	82	49.40	0.79	18.30	8.90	7.33	0.14	10.54	2.64	0.30	0.13	1.41	99.88	6	126	473	79	281	34	2.0	45
96022302	basalt	60	49.25	0.63	18.09	8.18	8.16	0.16	12.85	1.93	0.11	0.12	0.74	100.23	2	73	636	64	248	52	1.0	20

Sample	Y	Hf	U	Th	Pb	Ga	Cu	Zn	Sc	V	La	Ce	Pr	Nd	Sm	Eu	Gd	Tb	Dy	Ho	Er	Tm	Yb	Lu
Ardley and King George Islands																								
990114003	16	2.0	0.8	2.0	5	22	74	87	17	213	10.30	24.00	n.d.	12.00	3.30	1.21	n.d.	0.61	n.d.	n.d.	n.d.	n.d.	1.30	0.18
990112001	11	n.d.	0.6	3.0	3	19	108	55	27	273	4.00	12.00	n.d.	9.00	n.d.	n.d.	n.d.	n.d.	n.d.	n.d.	n.d.	n.d.	n.d.	n.d.
990112003	19	n.d.	1.5	3.5	4	21	81	86	16	171	12.00	30.00	n.d.	17.00	n.d.	n.d.	n.d.	n.d.	n.d.	n.d.	n.d.	n.d.	n.d.	n.d.
990112010	21	n.d.	1.0	4.5	9	22	101	95	22	211	14.00	35.00	n.d.	17.00	n.d.	n.d.	n.d.	n.d.	n.d.	n.d.	n.d.	n.d.	n.d.	n.d.
AF-5	10	1.0	0.6	2.5	5	20	64	31	26	167	6.24	13.88	1.70	8.76	2.15	0.63	1.57	0.27	1.86	0.30	0.93	0.14	1.06	0.16
AF-14	12	1.5	0.3	1.0	5	24	113	34	31	319	6.45	14.00	1.82	9.68	2.76	0.92	2.36	0.39	2.34	0.45	1.27	0.16	1.08	0.20
Greenwich Island																								
HA-1.1	13	1.0	0.2	1.0	5	23	5	11	26	73	5.22	12.17	1.61	8.72	2.19	0.94	2.05	0.39	2.46	0.44	1.26	0.16	1.47	0.20
HA-8.2A	24	6.5	2.8	5.8	12	18	100	57	18	160	18.81	40.42	4.44	20.94	5.06	1.13	4.97	0.81	4.51	0.90	2.83	0.40	2.84	0.45
HA-19.1	26	6.5	n.d.	5.5	n.d.	n.d.	n.d.	n.d.	23	183	12.11	24.15	2.52	11.34	2.69	0.72	2.65	0.41	2.15	0.44	1.39	0.21	1.47	0.22
HA-20	22	4.0	1.5	8.8	8	16	42	71	12	90	17.39	34.86	3.60	16.19	3.62	0.98	3.66	0.61	3.13	0.64	1.95	0.29	2.03	0.34
HY-4	30	5.0	3.0	9.0	9	23	171	2	21	162	22.70	46.05	5.16	25.01	6.60	1.21	4.81	0.92	5.61	1.08	2.73	0.43	3.27	0.53
PA-8.1A	14	1.5	0.5	2.5	5	13	49	40	33	193	8.13	17.91	2.37	12.00	2.90	0.93	2.32	0.51	2.66	0.55	1.46	0.17	1.34	0.23
Livingston Island																								
98011501	27	2.0	0.2	1.0	5	21	140	88	43	442	6.30	15.30	2.24	11.70	3.60	1.43	4.30	0.70	4.60	1.00	3.00	0.45	2.80	0.44
98012002	20	2.0	0.2	1.0	5	17	33	57	31	273	7.20	17.30	2.47	12.30	3.60	1.28	3.70	0.60	3.50	0.70	2.00	0.31	2.00	0.29
98012202	10	1.0	0.2	1.0	5	15	57	53	27	237	4.50	10.70	1.50	7.60	2.10	0.87	2.10	0.30	1.80	0.40	1.00	0.14	0.90	0.13
98012301	36	4.5	1.0	5.0	7	19	10	91	24	97	18.50	40.80	5.31	25.70	6.10	1.83	6.60	1.00	6.10	1.30	3.60	0.55	3.40	0.55
98012501	25	3.0	n.d.	2.5	n.d.	n.d.	38	78	24	189	10.00	25.00	n.d.	16.00	3.70	1.26	3.98	0.58	4.72	0.96	2.65	n.d.	2.70	0.40
Robert Island																								
96020701	18	2.0	1.5	2.0	5	18	108	71	20	250	13.90	30.40	n.d.	18.30	4.46	1.30	n.d.	0.91	n.d.	n.d.	n.d.	n.d.	1.59	0.21
96022001	16	n.d.	1.0	0.5	2	19	72	65	28	270	3.00	15.00	n.d.	9.00	n.d.	n.d.	n.d.	n.d.	n.d.	n.d.	n.d.	n.d.	n.d.	n.d.
96022005	13	1.0	0.3	2.0	1	18	80	58	26	221	4.90	11.00	n.d.	6.24	2.08	0.79	n.d.	0.38	n.d.	n.d.	n.d.	n.d.	1.31	0.21
96022302	10	n.d.	1.5	2.5	2	18	83	61	34	270	5.00	20.00	n.d.	9.00	n.d.	n.d.	n.d.	n.d.	n.d.	n.d.	n.d.	n.d.	n.d.	n.d.

Major elements in wt.%, trace elements in ppm. Ages in Ma.
n.d.=not determined.

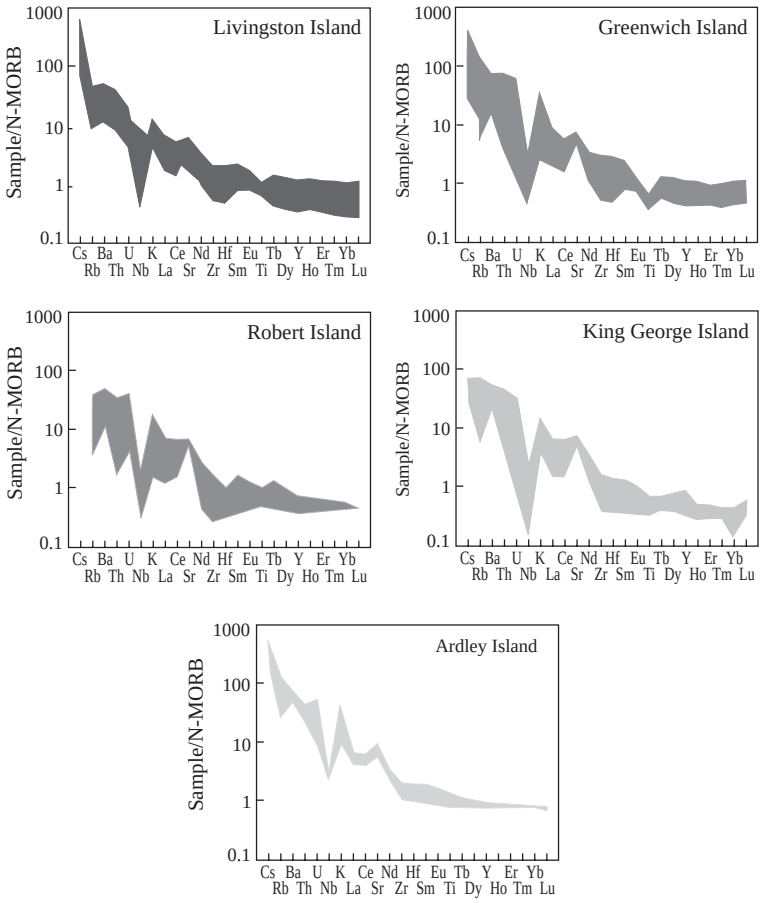

Fig. 7. Trace element variation diagrams for the studied South Shetland magmatic rocks, normalized to the N-type MORB of Sun and McDonough (1989).

Isotope data are summarized in Tables 2 and 3. Initial $^{87}Sr/^{86}Sr$ ratios vary from 0.7033 to 0.7046. Initial $(^{143}Nd/^{144}Nd)_o$ ratios are between 0.5127 and 0.5129, and εNd values vary from +2.71 to +7.30, which suggest asthenospheric mantle source for the analyzed samples. $^{208}Pb/^{204}Pb$ ratios vary from 38.12 to 38.70, $^{207}Pb/^{204}Pb$ ratios are between 15.49 and 15.68, and $^{206}Pb/^{204}Pb$ range from 18.28 to 18.81.

The Sr and Nd isotopic composition of the South Shetland samples broadly plot close to data of other arc magmas (Fig. 8), such as Aleutians, Kurile, Marianas, Tonga-Kermadec, Luzon, Lesser Antilles, Sunda and NE Japan. However, the South Shetland Arc magmas present lower εNd, and therefore lower $^{143}Nd/^{144}Nd$ ratios, than the Aleutians, Marianas, South Sandwich and N Lesser Antilles magmas.

5. Discussion and conclusions

The discussion that follows will try to better understand the source of the South Shetland Arc magmas through trace elements and mainly through isotopic data.

Experimental studies have shown that certain elements, such as Sr, Ba, U, and Pb, can be easily transported in a water-rich fluid, whereas other elements, such as Nb, Zr, and Ti, are normally much less mobile in this medium (Brenan et al.,

Table 2
Rb–Sr and Sm–Nd isotopic data for the studied plutonic and volcanic rocks from the South Shetland Islands

Sample	Lithology	Age	Rb (ppm)	Sr (ppm)	($^{87}Sr/^{86}Sr$)m	Error (in ppm)	$^{87}Rb/^{86}Sr$	($^{87}Sr/^{86}Sr$)I	Sm (ppm)	Nd (ppm)	$^{143}Nd/^{144}Nd$	Error (in ppm)	$^{147}Sm/^{144}Nd$	$\varepsilon Nd(t)$[a]
Ardley and King George Islands														
990114003	basaltic andesite	58	11	510	0.70362	20	0.06255	0.70357	4	18	0.51295	22	0.13436	6.58
990112001	basalt	58	6	672	0.70376	17	0.02589	0.70374	2	9	0.51294	10	0.13436	6.37
990112003	andesite	44	17	615	0.70360	20	0.08020	0.70355	4	17	0.51276	17	0.14226	2.78
990112010	basaltic andesite	58	23	593	0.70340	18	0.11201	0.70331	4	17	0.51292	10	0.14226	5.91
AF-5	basalt	58	9	551	0.70337	10	0.04632	0.70333	3	9	0.51300	11	0.14839	7.30
AF-14	basalt	58	4	636	0.70347	23	0.01997	0.70346	3	10	0.51297	14	0.15353	6.72
Greenwich Island														
HA-1.1	basalt	98	9	736	0.70384	9	0.03449	0.70379	3	10	0.51292	10	0.15878	5.87
HA-8.2A	tonalite	80	47	476	0.70399	14	0.28634	0.70367	5	21	0.51290	8	0.14395	5.62
HA-19.1	basalt	98	25	491	0.70399	17	0.14766	0.70379	3	11	0.51292	11	0.16489	5.90
HA-20	tonalite	80	54	443	0.70438	17	0.35350	0.70398	4	16	0.51284	12	0.15115	4.44
HY-4	tonalite	80	73	424	0.70411	14	0.49526	0.70354	6	25	0.51289	9	0.13909	5.35
PA-8.1A	gabbro	80	6	548	0.70404	9	0.02963	0.70400	3	11	0.51287	10	0.14821	4.90
Livingston Island														
98011501	basalt	115	8	461	0.70440	19	0.05033	0.70431	4	12	0.51287	12	0.20153	4.52
98012002	basalt	130	5	476	0.70413	28	0.03046	0.70407	4	12	0.51284	14	0.20153	3.92
98012202	basalt	115	5	574	0.70428	16	0.02526	0.70424	2	8	0.51288	8	0.15115	5.06
98012301	andesite	130	25	438	0.70460	18	0.16553	0.70429	6	26	0.51274	9	0.13952	2.71
98012501	basaltic andesite	130	22	369	0.70427	16	0.17290	0.70395	4	16	0.51282	16	0.15115	4.05
Robert Island														
96020701	basalt	82	13	538	0.70421	35	0.07007	0.70413	5	18	0.51280	42	0.15115	3.54
96022001	basalt	82	3	482	0.70402	23	0.01805	0.70400	2	9	0.51284	11	0.13436	4.55
96022005	basalt	82	6	473	0.70354	34	0.03372	0.70350	2	6	0.51284	10	0.20153	3.95
96022302	basalt	60	2	636	0.70383	25	0.00912	0.70382	2	9	0.51291	9	0.13436	5.84

Ages are in Ma.
[a] $\varepsilon Nd(t)=((^{143}Nd/^{144}Nd[sample,t]/^{143}Nd/^{144}Nd[CHUR,t])-1\times10^4$. For εNd^0 (today) assuming $^{143}Nd/^{144}Nd$ today=0.512638 ($^{146}Nd/^{144}Nd$=0.72190); $\varepsilon Nd^{(0)}=((^{143}Nd/^{144}Nd[sample,now]/0.512638)-1)\times10^4$.

1995). Recognition of this behavior has enabled the reconnaissance a separate fluid component (derived from the subducting slab itself) and a sedimentary component, introduced as partial melt, in the source of arc magmas (Ellam and Hawkesworth, 1988). These studies allow the affirmation that HFSE such as Zr and Nb are relatively insoluble in aqueous fluids, in contrast to LILE. Therefore, in island arc magmas, these elements are believed to be derived predominantly from the mantle wedge, and their relative high concentrations reflect the composition of the mantle wedge beneath the arc (Keppler, 1996). South Shetland Arc magmas show enrichment of LILE in samples from the island, following the sequence: Ardley > (Livingston and Greenwich) > (Robert and King George). The negative Nb and Zr anomalies obey the same sequence. Such evidence suggests that the source of the South Shetland Arc magmas has changed along time with more contribution from the subducting slab (e.g. Livingston Island–130 Ma) with high contents of LILE, to more contribution from the mantle material (e.g. King George Island–50 Ma) with high contents of HFSE.

εNd values together with ($^{87}Sr/^{86}Sr)_o$ ratios (Fig. 8) are compatible with absence of ancient, more

Table 3
Pb isotopic data of the studied plutonic and volcanic rocks from the South Shetland Islands

Sample	Lithology	Age	$^{206}Pb/^{204}Pb$	Error (%)	$^{207}Pb/^{204}Pb$	Error (%)	$^{208}Pb/^{204}Pb$	Error (%)
Ardley and King George Islands								
990114003	basaltic andesite	58	18.603	0.062	15.603	0.065	38.350	0.063
990112001	basalt	58	18.505	0.021	15.566	0.022	38.221	0.022
990112003	andesite	44	18.544	0.015	15.532	0.016	38.151	0.016
990112010	basaltic andesite	58	18.577	0.025	15.517	0.027	38.126	0.025
AF-5	basalt	58	18.555	0.006	15.568	0.005	38.254	0.013
AF-14	basalt	58	18.455	0.292	15.490	0.245	38.123	0.602
Greenwich Island								
HA-1.1	basalt	98	18.576	0.048	15.551	0.041	38.204	0.100
HA-8.2A	tonalite	80	18.687	0.026	15.577	0.025	38.415	0.025
HA-19.1	basalt	98	18.697	0.026	15.568	0.026	38.437	0.025
HA-20	tonalite	80	18.712	0.042	15.608	0.044	38.534	0.045
HY-4	tonalite	80	18.709	0.005	15.592	0.005	38.438	0.011
PA-8.1A	gabbro	80	18.634	0.006	15.573	0.005	38.343	0.011
Livingston Island								
98011501	basalt	115	18.560	0.018	15.593	0.017	38.354	0.017
98012002	basalt	130	18.591	0.023	15.570	0.021	38.311	0.020
98012202	basalt	115	18.567	0.033	15.582	0.033	38.254	0.034
98012301	andesite	130	18.808	0.086	15.677	0.089	38.703	0.089
98012501	basaltic andesite	130	18.281	0.027	15.609	0.028	38.179	0.029
Robert Island								
96020701	basalt	82	18.409	0.062	15.630	0.066	38.404	0.082
96022001	basalt	82	18.513	0.025	15.615	0.025	38.388	0.025
96022005	basalt	82	18.527	0.028	15.606	0.028	38.329	0.028
96022302	basalt	60	18.508	0.019	15.571	0.019	38.223	0.019
NBS 981 (n=9)	standard		16.893	0.0109	15.442	0.0119	36.558	0.0133
NIST[a]	standard		16.937	0.0011	15.941	0.0015	36.721	0.0036

Ages are in Ma.
[a] Data from Walder et al. (1993).

radiogenic continental crust involved in the formation of the South Shetland magmas, which suggest that any contribution of LILE could not be originated from an old lithosphere. The studied samples show changes in their isotope composition with time, the oldest rocks having the lowest εNd (Table 2, Fig. 8). Such feature ratifies the modification of the source of the magmas with time. Such change could also account changes in the composition of the subducted material that would be mixed with the mantle and result different its isotopic characteristics along time.

The Sr, Nd and Pb isotopic data for the studied samples are represented in Figs. 8–10. In Fig. 9($^{87}Sr/^{86}Sr$ vs. $^{143}Nd/^{144}Nd$) samples form a trend from the depleted MORB mantle (DMM) field to enriched mantle II (EMII) field. However, a secondary trend towards the enriched mantle I (EMI) is also suggested by some King George and Robert islands samples. $^{206}Pb/^{204}Pb$ vs. $^{208}Pb/^{204}Pb$ and $^{206}Pb/^{204}Pb$ vs. $^{207}Pb/^{204}Pb$ (Fig. 10a,b) shows that most samples form a trend from the DMM field toward the EMII field, except for two samples (one from the Robert Island and another one from the Livingston island) that plot outside this major trend. The observed moderate enrichments of ^{207}Pb and ^{208}Pb suggest involvement of sedimentary rocks in the mantle source. These isotopic compositions could be explained by variations in the composition of melt and/or fluids, or variations in the composition of the sedimentary rocks, or even a combination of both.

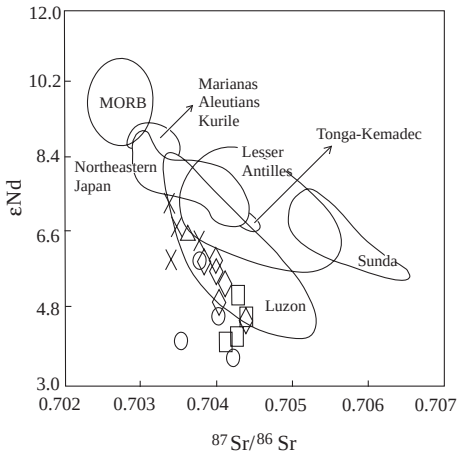

Fig. 8. Isotopic signature of the South Shetland Meso-Cenozoic magmatic rocks compared with other island arcs. Aleutians (Morris and Hart, 1983); Kurile (Zhuravlev et al., 1987); Marianas (Woodhead, 1989); Tonga-Kermadec (Regelous et al., 1997); Luzon (Chen et al., 1990); Lesser Antilles (Macdonald et al., 2000); Sunda (Stolz et al., 1990) and NE Japan (Shibata and Nakamura, 1997).

These Sr–Nd–Pb-isotope diagrams (Figs. 8–10) suggest a combination of DMM and EM II (and in a less extent EM I) as major source for the studied South Shetland magmas. This behavior could be explained by contamination of large volume of magma derived from the depleted asthenospheric mantle (DMM) with lithospheric fluids enriched in LILE and radiogenic Sr generated mainly from dehydration of detritic sediments during the subduction (EM II), and secondarily from pelagic sediments (EM I). As there is no trend towards the HIMU (high $^{238}U/^{204}Pb$ mantle) field in Fig. 10a,b and due to the values of εNd, we argue that oceanic crust is not contributing to the isotopic composition of the source. The contribution from the EM II is more important in the beginning of the volcanic events (Livington Island–130 Ma) and less important in the end (King George Island–50 Ma), in which EM I contribution is also important.

DMM is generally assigned to the upper mantle and is considered to be source of N-type MORB basalts. Since it is highly depleted in LILE and other incompatible elements, and characterized by non-radiogenic Sr but radiogenic Nd isotope ratios, DMM is commonly assumed to represent the refractory residue of previous events of magma extraction (Hofmann et al., 1986; Hart, 1988).

EM II component in the source of the studied rocks can be interpreted inherited from recycled continental crust (e.g. Zindler and Hart, 1986). EM I

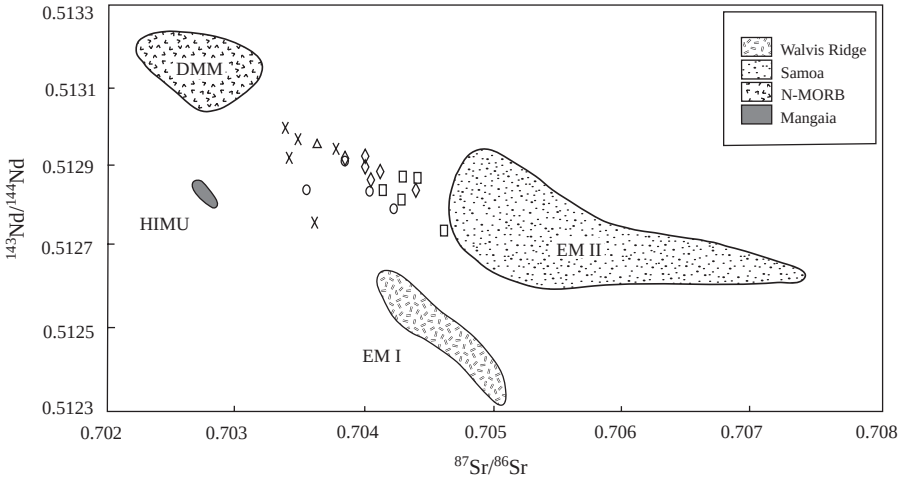

Fig. 9. Variation of $^{87}Sr/^{86}Sr$ and $^{143}Nd/^{144}Nd$ of the studied igneous rocks from South Shetland Arc compared with representative compositions of mantle end members. Data sources: Walvis Ridge, for DMM (depleted mantle) is from Richardson et al. (1982); Tutuila and Upolu in Samoa, for EMII (Enriched mantle II) is from Wright and White (1986/87); Palacz and Saunders (1986) and Farley et al. (1992); Mangaia, for HIMU (high μ) is from Palacz and Saunders (1986); and Atlantic N-MORB, for EM I (Enriched mantle I) is from Ito et al. (1987), with the exception of sample P6906-28B. Symbols: □=Livingston Island; ◇=Greenwich Island; ○=Robert Island; ×=King George Island and △=Ardley Island.

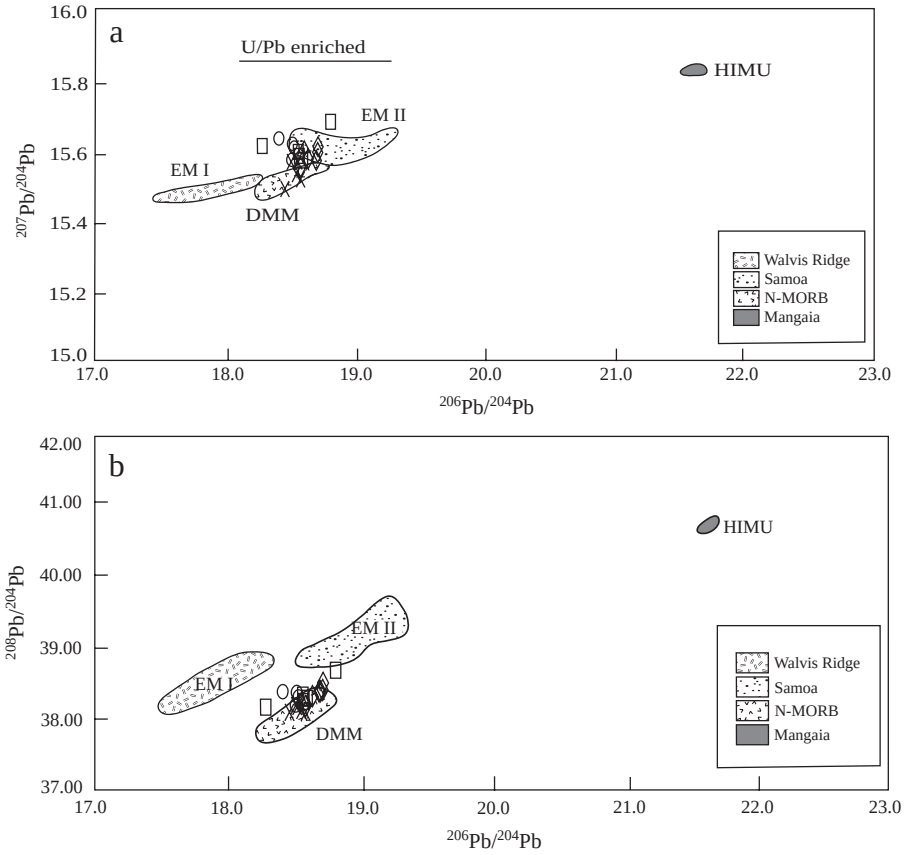

Fig. 10. Pb-isotope diagrams of the studied igneous rocks from South Shetland Arc. Compositional fields were defined on data from the literature as listed in the caption of Fig. 5. Symbols as in Fig. 9.

is not an important component for the samples analysed here, except in the younger volcanic events (around 50 Ma). Such component could be explained by: (i) recycling and ageing of pelagic sediments together with underlying oceanic crust (e.g. Weaver, 1991; Chauvel et al., 1992; Hémond et al., 1994), (ii) delamination or thermal erosion of subcontinental lithosphere that became part of the convecting upper mantle (e.g. Hoernle et al., 1991; Anderson, 1994), or (iii) metasomatism of lithosphere during subduction processes (e.g. Liu et al., 1994; Chung et al., 1995).

Modeling using the Sr and Nd content and the Sr and Nd isotopic composition (Fig. 11) indicates that the majority of samples can be explained by mixing between ≈96 wt.% of melts with N-MORB characteristics (from DMM source) and ≈4% of sedimentary end member, isotopically similar to the Pacific sediment (the detrital sediments-EM II). Modeling was done using the two-end-member assumption described in Faure (1986) following the equation described bellow, the Sr and Nd concentrations and Sr and Nd isotopic composition of an N-MORB (Cohen et al., 1980) estimated as originated from 10% of a depleted mantle (DMM) melting. The results are displayed in Table 4 and the equation is:

$$R^x_M = \frac{R^x_A X_A f + R^x_B X_B (1-f)}{X_A f + X_B (1-f)}$$

where R^x_M is na isotope ratio of X in a mixture of components A and B, X_A and X_B are concentrations

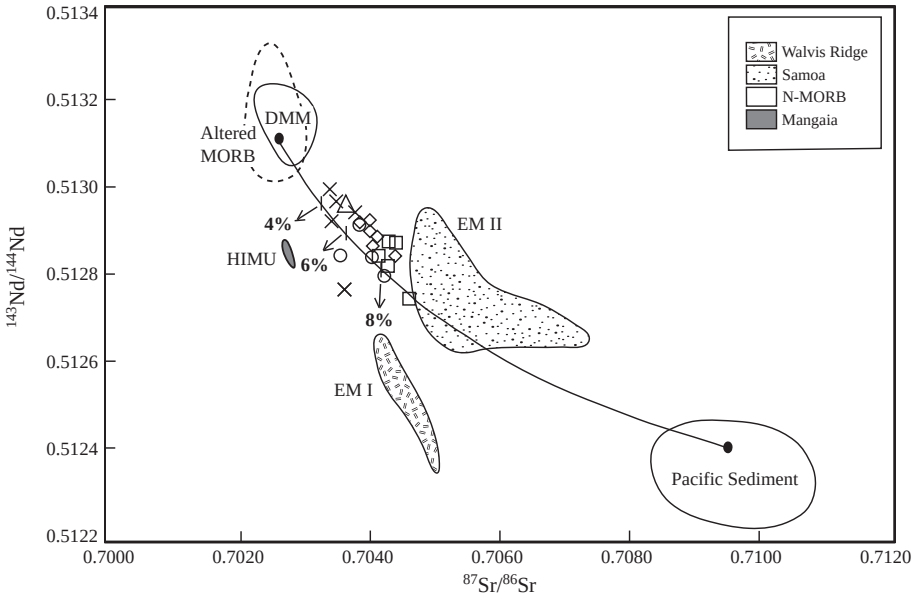

Fig. 11. Estimation of the isotopic composition of the subduction component as discussed in the text. The continuous curved line represents a mixing between altered MORB (DMM field) and sediments (Pacific sediments filed). It indicates the bulk mixture between 4 wt.% of sediment and 96 wt.% of altered MORB. The isotopic ratios of Sr and Nd of the sediments are from Othman et al. (1989). Symbols and fields as in Fig. 5. The dashed field next to the DMM field is the altered MORB filed, which represent the effect of alteration by seawaters on the DMM.

of X in A and B, and f is the weight fraction of A defined as:

$$f = \frac{A}{A+B}$$

where A and B are the weight of the two components in a given mixture.

On $^{206}Pb/^{204}Pb$ versus $^{207}Pb/^{204}Pb$, and $^{206}Pb/^{204}Pb$ versus $^{208}Pb/^{204}Pb$ diagrams (Fig. 10A,B) moderate enrichment in ^{207}Pb and ^{208}Pb is observed, which imply involvement of sedimentary material in the source. It is not possible to demonstrate unequivocally whether the isotope systematics are best explained by variations from the melt and/or fluids composition or variations in the composition of the sediment, or even a combination of both. Both processes are likely to have been active, and the question of their relative importance still remains open until more data is available.

Table 4
Sr, Nd and Pb isotopic ratios, and Sr, Nd and Pb concentrations of altered MORB and Pacific sediments used as en members for the modeling of the isotopic characteristics of the subducted component as discussed in the text and shown in Fig. 11

	$^{87}Sr/^{86}Sr$	$^{143}Nd/^{144}Nd$	$^{206}Pb/^{204}Pb$	Sr (ppm)	Nd (ppm)	Pb (ppm)
Altered MORB	0.70260	0.51310	18.480	114	17	0.54
Pacific Sediment	0.70950	0.51240	18.700	329	116	110

Acknowledgements

This research was supported by the Brazilian Antarctic Program (PROANTAR-CNPq), CAPES (Doctoral Sandwich Program scholarship at Federal University of Adelaide, Australia), Chilean Antarctic Institute (INACH; Projects 01-95, 03-96), and Antarctic Institutional Program of the University of Chile. We thank John Stanley (University of Adelaide, Australia), David Bruce (University of Adelaide, Australia) and Ana Maria Graciano Figueiredo (IPEN, Brazil) for analytical support during data acquisition. We thank also Francisco Hervé Allamand (University of Chile) and Delia del Pilar Montecinos de Almeida (UNISINOS) for donation of some Antarctic samples analyzed in this study. We also thank the important

comments and suggestions of the anonymous reviewers and guest editors.

References

Anderson, D.L., 1994. The sublithospheric mantle as the source of continental flood basalts; the case against the continental lithosphere and plume head reservoirs. Earth Planet. Sci. Lett. 123, 269–280.

Azevedo, G.C., 1992. Caracterização geológica, geoquímica e geocronológica da Ilha Dee e parte da Ilha Greenwich, Arquipélago das Shetland do Sul, Antártica. M.Sc. Thesis. Federal University of Rio Grande do Sul. 184 pp.

Barker, P.F., Burrell, J., 1977. The opening of Drake Passage. Mar. Geol. 25 (1/3), 15–34.

Barker, P.F., Dalziel, I.W.D., Storey, B.C., 1991. Tectonic development of the Scotia Arc region. In: Tingey, R.J. (Ed.), Antarctic Geology. Oxford University Press, Oxford, pp. 215–248.

Birkenmajer, K., Delitala, M.C., Narebski, W., Nicoletti, M., Petrucciani, C., 1986. Geochronology of Tertiary island-arc volcanics and glaciogenic deposits, King George Island, South Shetland Islands (West Antarctica). Pol. Acad. Sci. Earth Sci. 34, 257–273.

Brenan, J.M., Shaw, H.F., Ryerson, F.J., Phinney, D.L., 1995. Mineral-aqueous fluid partitioning of trace elements at 900 degrees C and 2.0 GPa: constraints on the trace element chemistry of mantle and deep crustal fluids. Geochim. Cosmochim. Acta 59, 3331–3350.

Chauvel, C., Hofmann, A.W., Vidal, P., 1992. HIMU-EM: the French Polynesian connection. Earth Planet. Sci. Lett. 110, 99–119.

Chen, C.H., Shieh, Y.N., Lee, T., Chen, C.H., Mertzman, S.A., 1990. Nd–Sr–O isotopic evidence for source contamination and an unusual mantle component under Luzon arc. Geochim. Cosmochim. Acta 54, 2473–2483.

Chung, S.-L., Jahan, B.-M., Chen, S.-J., Lee, T., Chen, C.-H., 1995. Miocene basalts in northwestern Taiwan: evidence for EM-type mantle sources in the continental lithosphere. Geochim. Cosmochim. Acta 59, 549–555.

Cohen, R.S., Evensen, N.M., Hamilton, P.J., O'Nions, R.K., 1980. U–Pb, Sm–Nd and Rb–Sr systematics of ocean ridge basalt glasses. Nature 283, 149–153.

Dalziel, I.W.D., 1984. Tectonic evolution of a forearc terrane, Southern Scotia Ridge. Geol. Soc. Am., Spec. Pap., vol. 200. 32 pp.

Ellam, R.M., Hawkesworth, C.J., 1988. Elemental and isotopic variations in subduction related basalts: evidence for a three component model. Contrib. Mineral. Petrol. 98, 72–80.

Farley, K.A., Natland, J.H., Craig, H., 1992. Binary mixing of enriched and undegassed (primitive?) mantle components (He, Sr, Nd, Pb) in Samoan lavas. Earth Planet. Sci. Lett. 111, 183–199.

Faure, G., 1986. Principles of Isotopic Geology. John Wiley and Sons, Inc., New York. 589 pp.

Figueiredo, A.M.G., Marques, L.S., 1989. Determination of rare earths and other trace elements in the Brazilian Geological Standards BB-1 and GB-1 neutron activation analysis. Geochim. Bras. 3, 1–8.

Gracanin, T.M., 1983. Geochemistry and geochronology of some Mesozoic igneous rocks from the northern Antarctic Peninsula region. M. Sc. Thesis. Ohio State University.

Grikurov, G.E., Krylov, A., Polyakov, M.M., Covbun, N., 1970. Vozrast gornych porod v severnoj casti Antarkticeskogo Poluostrova i na Juznych Setlandskich ostrovach (po dannyum kalij-argonovogo metoda). Inf. Biul. Sov. Antarkt. Eksped. 80, 30–33.

Hart, S.R., 1988. Heterogeneous mantle domains: signatures, genesis and mixing chronologies. Earth Planet. Sci. Lett. 90, 273–296.

Hathway, B., 1997. Nonmarine sedimentation in an Early Cretaceous extensional continental-margin arc, Byers Peninsula. Livingston Island, South Shetland Islands. J. Sediment. Res. 67, 686–697.

Hémond, C., Devey, C.W., Chauvel, C., 1994. Source compositions and melting processes in the Society and Austral plumes (South Pacific Ocean): element and isotope (Sr, Nd, Pb, Th) geochemistry. Chem. Geol. 115, 7–45.

Hoernle, K., Schmincke, H.-U., Tilton, G., 1991. Sr, Nd and Pb isotope geochemistry of volcanics from Madeira and Porto Santo Islands, North Atlantic Ocean. Eos 72, 528.

Hofmann, A.W., Jochum, K.P., Seufert, M., White, W.M., 1986. Nb and Pb in oceanic basalts: new constraints on mantle evolution. Earth Planet. Sci. Lett. 79, 33–45.

Ishikawa, T., Nakamura, E., 1994. Origin of the slab component in arc lavas from across-arc variation of B and Pb isotopes. Nature 370, 205–208.

Ito, E., White, W.M., Gopel, C., 1987. The O, Sr, Nd and Pb isotope geochemistry of MORB. Chem. Geol. 62, 157–172.

Jwa, Y.J., Park, B.K., Kim, Y., 1991. Geochronology and geochemistry of the igneous rocks from Barton and Fildes Peninsulas, King George Island: a review. In: Yoshida, Y., Kaminuma, K., Shiraishi, K. (Eds.), Recent progress in Antarctic Earth science. Terra Scientific Publishing Company, pp. 439–442.

Keller, R.A., Fisk, M.R., White, W.M., Birkenmajer, K., 1991. Isotopic and trace element constraints on mixing and melting models of marginal basin volcanism, Bransfield Strait, Antarctica. Earth Planet. Sci. Lett. 111, 287–303.

Keppler, H., 1996. Constraints from partitioning experiments on the composition of subduction-zone fluids. Nature 380, 237–240.

Lawver, A.L., Sloan, B.J., Barker, D.H.N., Ghidella, M., Von Herzen, R.P., Keller, R.A., Klinkhammer, G.P., Chin, C.S., 1996. Distributed, active extension in Bransfield Basin, Antarctic Peninsula: evidence from multibeam bathymetry. GSA Today 6 (11), 1–5.

Liu, C., Masuda, A., Xie, G., 1994. Major- and trace-element compositions of Cenozoic basalts in Eastern China: petrogenesis and mantle source. Chem. Geol. 114, 19–42.

Macdonald, R., Hawkesworth, C.J., Heath, E., 2000. The Lesser Antilles volcanic chain: a study in arc magmatism. Earth Sci. Rev. 49 (1–4), 1–76.

Machado, A., 1997. Petrologia, Geoquímica e Geologia Estrutural da Península Fildes. Ilha Rei George, Antártica, M.S. thesis, Fed. Univ. of Rio Grande do Sul, Brazil. 182 pp.

McCarron, J.J., Larter, R.D., 1998. Late Cretaceous to early Tertiary subduction history of the Antarctic Peninsula. J. Geol. Soc. London 155, 255–268.

Morris, J.D., Hart, S.R., 1983. Isotopic and incompatible element constraints on the genesis of island arc volcanics: Cold Bay and Amak Islands, Aleutians. Geochim. Cosmochim. Acta 47, 2015–2030.

Oteiza, O., 1999. Petrogénesis del magmatismo básico del Meso-Cenozoico en la Península Byers, Isla Livingston (Archipiélago de Shetland del Sur, Antártica). Graduation Degree. University of Chile, Chile, p. 100.

Othman, D.B., White, W.M., Patchett, J., 1989. The geochemistry of marine sediments, island arc magma genesis, and crust-mantle recycling. Earth Planet. Sci. Lett. 94, 1–21.

Palacz, Z.A., Saunders, A.D., 1986. Coupled trace element and isotope enrichment in the Cook-Austral-Samoa islands, south-west Pacific. Earth Planet. Sci. Lett. 79, 270–280.

Pankhurst, R.J., Riley, T.R., Fanning, C.M., Kelley, S.P., 2000. Episodic silicic volcanism in Patagonia and the Antarctic Peninsula: chronology of magmatism associated with the break-up of Gondwana. J. Petrol. 41 (5), 605–625.

Regelous, M., Collerson, K.D., Ewart, A., Wendt, J.I., 1997. Trace element transport rates in subduction zones: evidence from Th, Sr and Pb isotope data for Tonga-Kermadec arc lavas. Earth Planet. Sci. Lett. 150, 291–302.

Richardson, S.H., Erlank, A.J., Duncan, A.R., Reid, D.L., 1982. Correlated Nd, Sr, Pb isotope variation in Walvis Ridge Basalts and implications for the evolution of their mantle sources. Earth Planet. Sci. Lett. 59, 327–342.

Ryan, J.G., Morris, J., Tera, F., Leeman, W.P., Tsvetkov, A.W.P., 1995. Cross-arc geochemical variations in the Kurile arc as a function of slab depth. Science 270, 625–627.

Scambelluri, M., Philippot, P., 2001. Deep fluids in subduction zones. Lithos 55 (1–4), 213–227.

Shibata, T., Nakamura, E., 1997. Across-arc variations of isotope and trace element compositions from Quaternary basaltic volcanic rocks in northeastern Japan: implications for interaction between subducted oceanic slab and mantle wedge. J. Geophys. Res. 102 (B4), 8051–8064.

Smellie, J.L., Pankhurst, R.J., Thomson, M.R.A., Davies, R.E.S., 1984. The geology of the South Shetland Islands: VI. Stratigraphy, geochemistry and evolution. British Antarctic Survey Reports, vol. 87. British Antarctic Survey and Natural Environment Research Council, Cambridge, 83 pp.

Stolz, A.J., Varne, R., Davies, G.R., Wheller, G.E., Foden, J.D., 1990. Magma source compositions in an arc-continent collision zone: the Flores-Lembata sector, Sunda arc, Indonesia. Contrib. Mineral. Petrol. 105, 585–601.

Sun, S.S., McDonough, W.F., 1989. Chemical and isotopic systematics of oceanic basalts: implications for mantle composition and processes. In: Saunders, A.D., Norry, M.J. (Eds.), Magmatism in the ocean basins, Geological Society of London, Special Publication, vol. 42, pp. 313–345.

Trouw, R.A.J., Passchier, C.W., Valeriano, C.M., Simões, L.S.A., Paciullo, V.P., Ribeiro, A., 2000. Deformational evolution of a Cretaceous subduction complex: Elephant Island, South Shetland Islands, Antarctica. Tectonophysics 319, 93–110.

Walder, A.W., Platzner, I., Freedman, P., 1993. Isotope ratio measurement of Lead, Neodymium and Neodymium-Samarium mixtures, Hafnium and Hafnium-Lutetium mixtures with a double focusing multiple collector inductively coupled plasma mass spectrometer. J. Anal. At. Spectrom. 8, 19–23.

Weaver, B.L., 1991. The origin of ocean island basalt end-member compositions: trace element and isotopic constraints. Earth Planet. Sci. Lett. 104, 381–397.

White, W.M., Dupre, B., 1986. Sediment subduction and magma genesis in the Lesser Antilles: isotopic and trace element constraints. J. Geophys. Res. 91, 5927–5941.

Woodhead, J.D., 1989. Geochemistry of the Mariana arc (western Pacific): source composition and processes. Chem. Geol. 76, 1–24.

Woodhead, J., Eggins, S., Gamble, J., 1993. High field strength and transition element systematics in island arc and back-arc basin basalts: evidence for multi-phase melt extraction and a depleted mantle wedge. Earth Planet. Sci. Lett. 114, 491–504.

Wright, E., White, W.M., 1986/87. The origin of Samoa: new evidence from Sr, Nd, and Pb isotopes. Earth Planet. Sci. Lett. 81, 151–162.

Zhuravlev, D.Z., Andrei, A.T., Zhuravlev, A.Z., Gladkov, N.G., Chernyshev, I.V., 1987. $^{143}Nd/^{144}Nd$ and $^{87}Sr/^{86}Sr$ ratios in recent magmatic rocks of the Kurile island arc. Chem. Geol. 66, 227–243.

Zindler, A., Hart, S.R., 1986. Chemical geodynamics. Annu. Rev. Earth Planet. Sci. 14, 493–571.